J. Fluid Mech. (1990), *vol.* 220, *pp.* 673–689
Printed in Great Britain

Absolute and convective instability of a liquid sheet

By S. P. LIN, Z. W. LIAN AND B. J. CREIGHTON
Department of Mechanical and Aeronautical Engineering, Clarkson University, Potsdam, NY 13676, USA

(Received 1 September 1989)

The linear stability of a viscous liquid sheet in the presence of ambient gas is investigated. It is shown that there are two independent modes of instability, sinuous and varicose. The large-time asymptotic amplitude of sinuous disturbances is found to be bounded but non-vanishing for all calculated values of Reynolds numbers and the gas-to-liquid density ratios when the Weber number is greater than one half. The Weber number W_e is defined as the ratio of the surface tension force to the inertia force per unit area of the gas–liquid interface. When W_e is smaller than one half, the sinuous mode is stable if the gas-to-liquid density ratio is zero, otherwise it is convectively unstable. The varicose mode is always convectively unstable unless the density ratio, Q, is zero. Then it is asymptotically stable. The spatial growth rate of the varicose mode is smaller than that of the sinuous mode for the same flow parameters. The wavelength of the most amplified waves in both modes is found to scale with the product of the sheet thickness and Q/W_e. It is shown, by use of the energy equation, that the mechanism of instability is a capillary rupture when $W_e \geqslant 0.5$, and the convective instability is due to the interfacial pressure fluctuation when $W_e < 0.5$.

1. Introduction

The dynamics of thin sheets of liquids was studied by G. I. Taylor (1959*a*, *b*, *c*), and the disintegration of liquid sheets in the context of atomization has been investigated by Clark & Dombrowski (1972), Crapper *et al.* (1973), Crapper, Dombrowski & Pyott (1975) and Weihs (1978). Brown (1961), Lin (1981) and Lin & Roberts (1981) studied the stability of liquid sheets formed by extrusion, which are encountered in curtain coating applications. A thin sheet of viscous liquid flowing between two vertical guide wires is an integral part of a process called curtain coating. Some descriptions of this process and its applications in various industries can be found in the references cited above. Lin showed that in the absence of ambient gas, the viscous liquid curtain is asymptotically stable with respect to temporally or spatially growing disturbances when the Weber number is smaller than one half. The Weber number is defined here as the ratio of the surface tension force to the inertia force per unit area of the free surface. Lin predicted the wave speeds of two distinctive modes of disturbances which exhibit themselves in the form of sinuous and varicose waves. These waves were observed by Lin & Roberts (1981) and Antoniades & Lin (1980). They also exploited the wave properties in a stable liquid curtain to experimentally determine the value of dynamic surface tension on a rapidly moving free surface. Kistler & Scriven (1984) investigated the curtain coating flow numerically by use of finite-element methods.

In the theoretical works cited above, the effect of the ambient gas is completely neglected. On the other hand, all of the experimental works cited above were carried

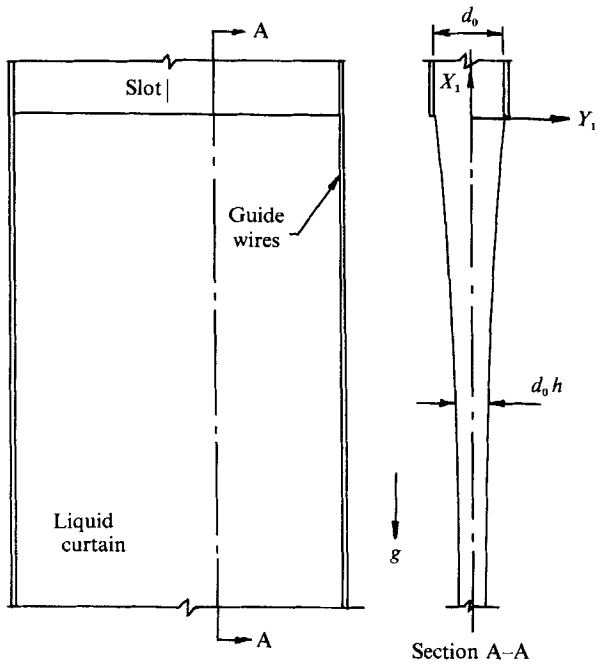

FIGURE 1. Definition sketch.

out in the presence of the ambient gas. Moreover, Taylor (1963) showed in his study of the ripple formation on an infinitely thick viscous circular jet that the ambient gas may have the effect of decreasing the interfacial wavelength by orders of magnitude even if the gas viscosity is neglected. If this is also true for viscous sheets, then the effect of the ambient gas is of great importance in many applications, including curtain coatings and fuel atomization by the use of sheets formed from various industrial devices. The results of the solution to the problem formulated in §2 showed that this is indeed the case. It is shown that when the Weber number is smaller than 0.5, the sheet is convectively unstable unless it is in vacuum. Then it is asymptotically stable. When $W_e \geqslant 0.5$, the sheet is convectively stable in a vacuum for finite wavelength of disturbances but pinch-point singularity is encountered at zero wavenumber. The physical mechanisms of instability are sought from an energy balance carried out in §3, and are expounded in the light of numerical results given in §4. The practical implications of the results are discussed in the final section.

2. Stability analysis

Consider the steady flow in a Newtonian liquid sheet, which is extruded vertically downward, as shown in figure 1. Assuming that the flow is essentially two-dimensional and that the effects of surface tension and the ambient gas as well as the normal stress variation across the sheets are negligible, Taylor derived the following dimensionless differential equation for the velocity variation in the liquid sheet:

$$(U_X/U)_X - U_X - U^{-1} = 0, \quad U_X + V_Y = 0, \tag{1}$$

where U and V are the dimensionless velocity components in the directions of the Cartesian coordinates X and Y respectively, and the subscripts denote differentiation.

The derivation of (1) can be found in the work of Brown (1961). It should be pointed out that the sign of the last term in the first equation of (1) is opposite to that of the corresponding term in Taylor's equation, owing to the opposite direction of the X-axis used here. The dimensionless quantities appearing in (1) are related to their dimensional counterparts (U_1, V_1) and (X_1, Y_1) by

$$(U_1, V_1) = (4\mu_1 g/\rho_1)^{\frac{1}{3}}(U, V), \quad (X_1, Y_1) = (4\mu_1/\rho_1)^{\frac{2}{3}} g^{-\frac{1}{3}}(X, Y),$$

where μ_1 and ρ_1 are respectively the dynamic viscosity and density of the liquid, and the distance X_1 is measured from the upper edge of the sheet in the direction opposite to that of the gravitational acceleration g. Brown found good agreement between the numerical solution of (1) and his measured velocities, except near the outlet of the fluid feeder, when the sheet is extremely thin. Moreover, in a certain parameter range, the velocity in the sheet is essentially uniform.

In the present stability analysis, the distance will be non-dimensionalized with the maximum sheet thickness d_0, and the velocity will be non-dimensioanlized with the average velocity $U_0 = \dot{Q}/d_0$, $\dot{Q}$ being the volumetric flow rate per unit width of the sheet. Denoting the new dimensionless basic state velocity and the Cartesian coordinates respectively by $(\bar{u}, \bar{v})$ and (x, y), we have

$$\left.\begin{aligned} &\bar{u}_x = \delta U_X = -\bar{v}_y, \\ &\delta = \left(\frac{R}{4F^2}\right)^{\frac{1}{3}} = \left(\frac{g^2}{4\nu}\right)^{\frac{1}{3}} \frac{d_0^2}{\dot{Q}}, \\ &R = \frac{\rho_1 U_0 d_0}{\mu_1} \equiv \text{Reynolds number}, \\ &F = \frac{U_0^2}{g d_0} \equiv \text{Froude number}. \end{aligned}\right\} \tag{2}$$

According to figure 5 of Brown, $U_X = O(1)$. Thus for the case of thin sheets such that $\delta \ll 1$, the spatial variation in the basic-state velocity is much smaller than order one, according to (2). We consider here only the case of $\delta \ll 1$. This inequality is amply satisfied in many applications, including the atomization of fuel in diesel engines and film coating. In the film coating application, the viscous liquid sheet is extruded by a rapidly moving substrate upon which the sheet falls perpendicularly. For any given feed rate $\dot{Q}$ the sheet thickness may become so thin, owing to the fast moving substrate, that δ becomes much smaller than one. $\delta \ll 1$ implies that gravitational force is much smaller than viscous force, since δ represents the ratio of the former to the latter force. Following Taylor's (1963) treatment of a related problem, we neglect the viscosity of the ambient gas. This neglect of gas viscosity is based on the observation that the instability is caused by capillary waves which may be assisted by the pressure fluctuation at the interface, and also on the assumption that the gas viscosity is weakly stabilizing. This assumption is based on the finding of a related work by Tomotika (1934) who showed that the gas viscosity is stabilizing for a viscous liquid jet emerging into a quiescent gas. Hence the basic flow of the present stability problem is given by

$$(U_1, V_1) = (-U_0, 0), \quad (U_2, V_2) = (0, 0),$$

$$\bar{P}_1 = \bar{P}_2 = \text{constant}, \quad h = \pm 0.5 d_0,$$

where the subscript 2 denotes the gas phase, $\bar{P}_1$ and $\bar{P}_2$ are the pressures in the liquid sheet and in the ambient gas respectively and h is the distance measured from the X_1-axis to the liquid–gas interface.

To investigate the stability, we perturb the basic flow with disturbances, and write the perturbed velocity and pressure fields respectively as

$$V_i = \bar{V}_i + v_i', \quad P_i = \bar{P}_i + p_i' \quad (i = 1, 2)$$

where primed quantities are perturbations, $i = 1$ stands for the liquid phase and $i = 2$ stands for the gas phase, and

$$\bar{V}_1 = (-U_0, 0), \quad \bar{V}_2 = (0, 0).$$

Substituting the perturbed velocity and pressure into the Navier–Stokes equations, subtracting out the basic state, and retaining only the terms of first order in perturbation, we have the following governing equations of the linear stability:

$$\left.\begin{aligned} (\partial_t - \delta_{i1} U_0 \partial_x) v_i' &= -(\nabla p_i')/\rho_i + \nu_i \nabla^2 v_i', \\ \nabla \cdot v_i' &= 0 \quad (i = 1, 2), \end{aligned}\right\} \tag{3}$$

where t is time, ρ_2 is the gas density, δ_{i1} is the Kronecker delta function and $\nu_2 = 0$. It should be pointed out that the gravitational force term is absent in (3), because it was subtracted out by the basic-state velocity and pressure fields. In terms of the following dimensionless variables:

$$\tau = \frac{t}{d_0/U_0}, \quad v_i = \frac{v_i'}{U_0} = (u_i, v_i), \quad \frac{\bar{V}_1}{U_0} = -i, \quad (x, y) = \frac{(X_1, Y_1)}{d_0}, \quad p_i = \frac{p_i'}{\rho_1 U_0^2},$$

(3) can be rewritten as

$$(\partial_\tau - \delta_{i1} \partial_x) v_i = -(\rho_1/\rho_i) \nabla p_i + (\delta_{i1}/R) \nabla^2 v_i, \tag{4}$$

$$\nabla \cdot v_i = 0. \tag{5}$$

In the linear theory, the boundary conditions need not be applied at the perturbed interfaces

$$\zeta = \pm 0.5 + \eta_\pm,$$

where η_+ and η_- are respectively the interfacial displacement from $y = 0.5$ and $y = -0.5$. We may expand all variables at the interface about $y = \pm 0.5$ by use of Taylor series, and retain only first-order terms in perturbations. In practice, the wave amplitude η must be even smaller than δ in order to allow the Taylor series expansion. However, in linear theory η is infinitesimal, and this requirement is satisfied. Hence we apply the expanded boundary conditions at $y = \pm 0.5$. From the balance of normal force per unit area of the interfaces at $\zeta = 0.5 + \eta_+$ and $\zeta = -0.5 + \eta_-$, we have

$$p_1 - p_2 \pm W_e(\eta_\pm)_{xx} - \frac{2v_{1,y}}{R} = 0, \tag{6a}$$

where $W_e = S/\rho_1 U_0^2 d_0$, S being the surface tension. The balance of tangential stress requires at $y = \pm 0.5$ that

$$v_{1,x} + u_{1,y} = 0. \tag{6b}$$

Since the interfaces are material surfaces, they must satisfy the kinematic boundary condition at $y = +0.5$,

$$v_i = \eta_{+,\tau} - \delta_{1i}\eta_{+,x} \quad (i = 1, 2); \tag{6c}$$

and at $y = -0.5$

$$v_i = \eta_{-,\tau} - \delta_{1i}\eta_{-,x} \quad (i = 1, 2). \tag{6d}$$

There are altogether eight boundary conditions in 6(*a–d*).

The two-dimensional normal mode solution of the governing differential system will be sought in the following form:

$$(v_i, u_i, p_i, \eta_\pm) = [\hat{v}_i(y), \hat{u}_i(y), \hat{p}_i(y), \hat{\eta}_\pm] \exp(\omega\tau + \mathrm{i}kx),$$

where ω and k are respectively the complex frequency and wavenumber of disturbances.

Taking the divergence of (4) and using the continuity equation (5), we have

$$\nabla^2 p_i = 0.$$

The bounded normal-mode solutions of this Laplace equation in the liquid sheet and the ambient gas yield the amplitudes of the pressure perturbations,

$$\hat{p}_1 = [(\mathrm{i}k - \omega)/k][A\cosh(ky) + B\sinh(ky)], \tag{7a}$$

$$\hat{p}_2 = -Q\omega F_+ \exp(-ky), \quad y > 0, k_r > 0; \qquad \hat{p}_2 = Q\omega F_+ \exp(ky), \quad y > 0, k_r < 0, \tag{7b, c}$$

$$\hat{p}_2 = -Q\omega F_- \exp(ky), \quad y < 0, k_r > 0; \qquad \hat{p}_2 = Q\omega F_- \exp(-ky), \quad y < 0, k_r < 0; \tag{7d, e}$$

where $Q = (\rho_2/\rho_1)$, k_r is the real part of k, and A, B, F_+ and F_- are integration constants. Only the characteristic equations for the case of $k_r > 0$ will be derived in detail. It will be shown that the characteristic equations for both cases remain essentially the same. The amplitudes of the disturbance velocity components can be obtained from (4) with p_i given by (7*a*), (7*b*) and (7*c*). They are

$$\left.\begin{aligned} \hat{v}_1 &= A\sinh(ky) + B\cosh(ky) + C\sinh(my) + D\cosh(my), \\ \hat{u}_1 &= \frac{\mathrm{i}}{k}[kA\cosh(ky) + mC\cosh(my) + kB\sinh(ky) + mD\sinh(my)], \end{aligned}\right\} \tag{8}$$

$$m = [k^2 + R(\omega - \mathrm{i}k)]^{\frac{1}{2}}, \quad \hat{v}_2 = \mp kF_\pm \exp(\mp ky), \quad \hat{u}_2 = \mathrm{i}kF_\pm \exp(\mp ky). \tag{9}$$

Substitution of the solutions obtained into the boundary conditions yields a system of eight linear homogenous equations in eight unknown components A, B, C, D, F_+, F_-, η and η_- of the eigenvector. These unknowns can be found directly from the eight equations. However, we shall exploit the fact that the odd and even eigensolutions are decoupled, and reduce the size of the system of equations.

For the odd solution of v_1, $B = D = 0$ in (8). The amplitudes of the interfacial displacements can be obtained from (6*c*) and (6*d*) with $i = 2$. They are

$$\hat{\eta}_\pm = \mp\frac{k}{\omega} F_\pm \exp(-\tfrac{1}{2}k). \tag{10}$$

It follows from (6*c*), (6*d*) and (8) that we have for the odd mode

$$(\omega - \mathrm{i}k)\,\hat{\eta}_\pm = \pm[A\sinh(\tfrac{1}{2}k) + C\sinh(\tfrac{1}{2}m)]. \tag{11}$$

This equation states that the two interfaces of the liquid sheets are displaced in opposite directions for the odd mode, i.e.

$$\hat{\eta}_+ = -\hat{\eta}_-. \tag{12}$$

Hence this mode will be termed the varicose mode. Substitution of (12) into (10) shows that

$$F_+ = F_- = F. \tag{13}$$

Substituting (7), (8), (10), (12) and (13) into the boundary conditions (6*a*), (6*b*) and (6*d*) with $i = 1$, we have respectively

$$A\left[\frac{ik-\omega}{k}-\frac{2k}{R}\right]\cosh(\tfrac{1}{2}k)-C\frac{2m}{R}\cosh(\tfrac{1}{2}m)+F\left[Q\omega+\frac{W_e k^3}{\omega}\right]\exp(-\tfrac{1}{2}k)=0,$$

$$A[2k^2\sinh(\tfrac{1}{2}k)]+C(m^2+k^2)\sinh(\tfrac{1}{2}m)=0,$$

and

$$A\sinh(\tfrac{1}{2}k)+C\sinh(\tfrac{1}{2}m)+(\omega-ik)\frac{k}{\omega}F\exp(-\tfrac{1}{2}k)=0.$$

It is straightforward to show that the solution of this system is given by

$$A=-\frac{k^2(m^2+k^2)\exp(-\tfrac{1}{2}k)F}{\omega R\sinh(\tfrac{1}{2}k)},\quad C=\frac{2k^3\exp(-\tfrac{1}{2}k)F}{\omega R\sinh(\tfrac{1}{2}m)}, \tag{14}$$

where the complex eigenfrequency ω and complex wavenumber k are related by the characteristic equation

$$Q\omega^2+W_e k^3+(m^2+k^2)R^{-2}\coth(\tfrac{1}{2}k)+\left(\frac{2}{R}\right)^2 k^3 m\coth(\tfrac{1}{2}m)=0. \tag{15}$$

Equation (15) was derived for the case of $k_r > 0$. It will be shown presently that for the case of $k_r < 0$, the characteristic equation remains (15) except that the sign of the first term is changed. It is clear that the pressure fields given in (7) for $k_r < 0$ affect only the solution for the gas phase. Because of the sign reversal in the exponent of the pressure expressions in (7) due to the change in sign of k_r, the signs of exponents in the exponential functions appearing in all equations between (7) and (14) must be reversed. In addition, the sign of Q must be changed since there is a difference in the sign of Q for different signs of k_r in (7). However, the exponential function is factored out in the final step of arriving at (15). Thus, the characteristic equation remains the same except that the sign of Q is changed. It will be seen that this change of sign of Q does not affect the results to be presented.

For the even-mode solution, $A = C = 0$. It follows from (8), (6*c*) and (6*d*) that the fluid particle velocities as well as the interfacial displacements at the two interfaces are in unison, i.e. $\hat{\eta}_+ = \hat{\eta}_-$, and $F_+ = F_-$. The algebra required to yield the eigenvectors and the secular equations for this sinuous mode is identical to that for the varicose mode, except that hyperbolic sine and tangent functions must respectively be replaced by the hyperbolic cosine and cotangent functions and vice versa. Thus the characteristic equation for the case of $k_r > 0$ is

$$Q\omega^2+W_e k^3+R^{-2}(m^2+k^2)\tanh(\tfrac{1}{2}k)+\left(\frac{2}{R}\right)^2 k^3 m\tanh(\tfrac{1}{2}m)=0, \tag{16}$$

and the eigenvector is given by

$$B = -\frac{k(m^2+k^2)\exp(-\frac{1}{2}k)}{\omega R\cosh(\frac{1}{2}k)}, \quad D = \frac{2k^3\exp(-\frac{1}{2}k)}{\omega R\cosh(\frac{1}{2}m)}; \tag{17}$$

here F is put equal to 1 without loss of generality. Again, (16) remains valid for $k_r < 0$, except that the sign of Q needs to be changed.

When $k \to \infty$, $[\coth(\frac{1}{2}k), \coth(\frac{1}{2}m), \tanh(\frac{1}{2}k), \tanh(\frac{1}{2}m)] \to 1$ and both (15) and (16) reduce to

$$Q\omega^2 + W_e k^3 + \frac{[2k^2+R(\omega-\mathrm{i}k)]^2}{R^2} - k^3\left(\frac{2}{R}\right)^2[k^2+R(\omega-\mathrm{i}k)]^{\frac{1}{2}} = 0. \tag{18}$$

This is the characteristic equation obtained by Taylor (1963) in his investigation of the generation of ripples by wind over an infinitely deep viscous fluid.

Identifying the wave frequency ω and the wavenumber k with the corresponding expressions in the work of Lin (1981), we have

$$\omega = \mathrm{i}\alpha c, \quad k = \alpha, \quad \omega - \mathrm{i}k = -\mathrm{i}\alpha(c+1) = \mathrm{i}\alpha c'.$$

Substituting these into (15) with $Q = 0$, we have

$$c'^2 + \frac{4\mathrm{i}\alpha c'}{R} - \frac{4\alpha^2}{R^2} - W_e\alpha\tanh(\tfrac{1}{2}\alpha) + \frac{4\alpha m}{R^2}\tanh(\tfrac{1}{2}\alpha)\coth(\tfrac{1}{2}m) = 0.$$

Multiplying this equation with $\mathrm{i}\alpha Rc'(m^2+\alpha^2)$ and rearranging terms, we have

$$c'^2 + c'\frac{2\mathrm{i}\alpha}{R}[1 - 2\alpha m(m^2+\alpha^2)^{-1}\coth(\tfrac{1}{2}m)\tanh(\tfrac{1}{2}\alpha) + W_e\alpha\tanh(\tfrac{1}{2}\alpha)[2\alpha^2(m^2+\alpha^2)^{-1}] = 0.$$

This is (13) of Lin (1981), with dimensionless sheet thickness $h = 1$ for the varicose mode in the absence of the ambient gas. Similarly (16) in this work with $Q = 0$ can be reduced to (17) of Lin's sinuous mode characteristic equation.

It should be emphasized that both k and ω are treated as complex in this work. The imaginary part of $k = k_r + \mathrm{i}k_i$ and the real part of $\omega = \omega_r + \mathrm{i}\omega_i$ give respectively the spatial and temporal growth of the disturbances. For the given flow parameters W_e, Q, R and given wavenumber–frequency pairs (k_r, ω_i), the values of (k_i, ω_r) will be obtained from the characteristic equations to determine the stability of the liquid sheet. It will be shown in §4 that the sheet may be absolutely or convectively unstable depending on the flow parameters. The numerical solution of the characteristic equations was accomplished by use of the Muller (1956) method.

3. Energy budget

In order to trace the energy sources of the absolute and convective instabilities, we balance the energy budget in a disturbed liquid sheet. Consider a control volume of the liquid per unit sheet width over one wavelength, $\lambda = 2\pi/k_r$, of the disturbance. Forming the dot product of (4) for liquid ($i = 1$) with $\boldsymbol{v}_1$, integrating over the control volume, using (5) and the Gauss theorem to reduce some of the volume integrals to surface integrals, we arrive at the energy equation (cf. Kelly *et al.* 1989; Creighton 1989)

$$\dot{K} = \dot{R} + \dot{I} + \dot{D}, \tag{19}$$

where, omitting the subscript 1 of the liquid phase,

$\dot{K} \equiv$ time rate of change of disturbance kinetic energy

$$= \int_{-\lambda}^{0} (\partial_\tau - \partial_x)\, e \, \mathrm{d}x, \quad e = \boldsymbol{v} \cdot \tfrac{1}{2}\boldsymbol{v};$$

$\dot{R} \equiv$ rate of reversible work

$$= -\int_{-\lambda}^{0} [pv]_{y=-0.5}^{y=0.5} \mathrm{d}x - \int_{-0.5}^{0.5} [pu]_{x=-\lambda}^{x=0} \mathrm{d}y;$$

$\dot{I} \equiv$ rate of irreversible work

$$= \frac{1}{R}\int_{-\lambda}^{0} [u(u_y + v_x) + 2vv_y]_{y=-0.5}^{y=0.5} \mathrm{d}x + \frac{1}{R}\int_{-0.5}^{0.5} [v(u_y + v_x) + 2uu_x]_{x=-\lambda}^{x=0} \mathrm{d}y;$$

$\dot{D} \equiv$ rate of energy dissipation by viscosity

$$= -\frac{2\pi}{R}\int_{-\lambda}^{0}\int_{-0.5}^{0.5} [(v_y)^2 + (u_x)^2 + \tfrac{1}{2}(u_y + v_x)^2] \, \mathrm{d}y \, \mathrm{d}x,$$

where $$[G(z)]_{z=b}^{z=a} \equiv [G(a) - G(b)].$$

The first term in the reversible work rate integral can be rewritten by applying the boundary condition (6*a*),

$$\int_{-\lambda}^{0} [pv]_{y=-0.5}^{y=0.5} \mathrm{d}x = \int_{-\lambda}^{0} \left[v\left(p_{2\mp} W_e (\eta_\pm)_{xx} + \frac{2v_y}{R} \right) \right]_{y=-0.5}^{y=0.5} \mathrm{d}x.$$

Note that in (19) the last term in the above integrand cancels the second term of the first integral in the expression of $\dot{I}$. Moreover, $(u_y + v_x)$ in the first integral of $\dot{I}$ vanishes by virtue of the boundary condition (6*b*). Henceforth it is understood that $\dot{I}$ consists of only the second integral in the above expression of $\dot{I}$, and $\dot{R}$ is now redefined as

$$\dot{R} = -\int_{-\lambda}^{0} [p_2 v_1]_{y=-0.5}^{y=0.5} \mathrm{d}x - \int_{-0.5}^{0.5} [pu]_{x=-\lambda}^{x=0} \mathrm{d}y + W_e \int_{-\lambda}^{0} [\pm v(\eta_\pm)_{xx}]_{y=-0.5}^{y=0.5} \mathrm{d}x.$$

The first integral represents the power $\dot{P}$ exerted by the gas pressure on the liquid sheet and the second integral represents the flow work rate at the top and bottom of the control volume. The third integral in $\dot{R}$ gives the surface tension work rate $\dot{S}$. Equation (19) can now be rewritten as

$$\dot{K} = \dot{P} + \dot{P}_{\mathrm{f}} + \dot{S} + \dot{I} + \dot{D}, \tag{20}$$

where $$\dot{P} = -\int_{-\lambda}^{0} [p_2 v_1]_{y=-0.5}^{y=0.5} \mathrm{d}x, \quad \dot{P}_{\mathrm{f}} = -\int_{-0.5}^{0.5} [pu]_{x=-\lambda}^{x=0} \mathrm{d}y,$$

$$\dot{S} = W_e \int_{-\lambda}^{0} [\pm v(\eta_\pm)_{xx}]_{y=-0.5}^{y=0.5} \mathrm{d}x.$$

It should be noted that the upper and lower signs in S are associated respectively with the surface at $y = 0.5$ and $y = -0.5$.

It is understood that the pressure and velocity components appearing in all integrals in this section are the real parts of their counterparts in §2. Each integral in (20) is evaluated with the adaptive Rombers (1984) method. To serve as a check

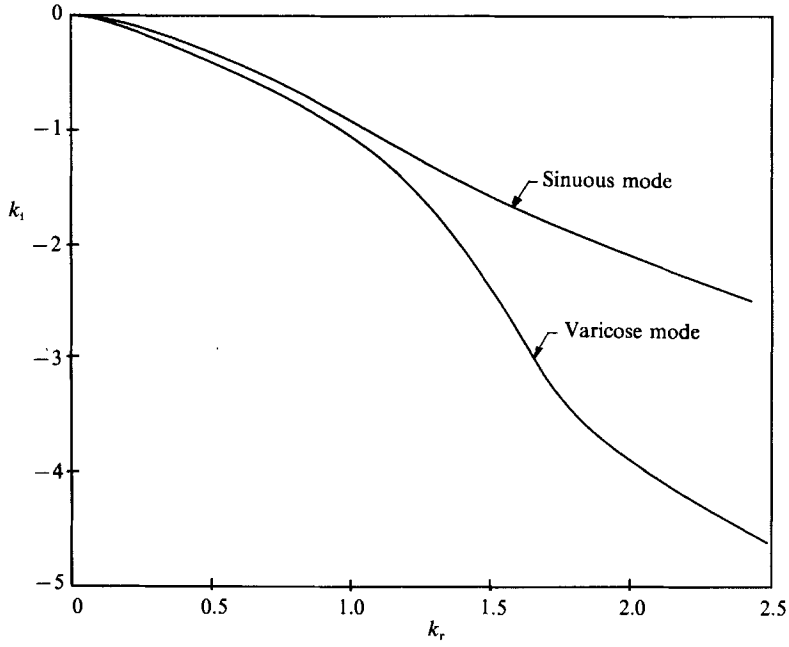

FIGURE 2. Stability of a liquid sheet. $Q = 0$, $W_e = 10^{-4}$, $R = 1$.

on the final accuracy, we add all integrals on the right-hand side of (20) and compare the result with the independently evaluated $\dot{K}$. The error is mostly less than 1 %. For a better appreciation of the relative importance of each item we shall present the energy budget in the variables defined below:

$$(\dot{p}, \dot{p}_\Gamma, \dot{s}, \dot{\tau}, \dot{d}) = [(\dot{P}, \dot{P}_\Gamma, \dot{S}, \dot{I}, \dot{D})/\dot{K}] \times 100.$$

4. Results and discussion

The spatial growth rate curves $\omega_r = 0$ for the sinuous and varicose disturbances in a liquid sheet at $Q = 0$, $W_e = 0.0001$ and $R = 1$ are given in figure 2. ω_i increases with k_r along these curves. Thus, the disturbance is convected downstream. Therefore, $k_i < 0$ on thes curves signifies that the sheet is convectively stable below the slot at the head of liquid sheet. These results confirm those obtained by Lin (1981) with a method of small-wavenumber expansion. He found that a liquid sheet in vacuum is stable if $W_e < 0.5$. However, in their experiments, Lin & Roberts (1981) and Antoniades & Lin (1980) observed that when $W_e > 0.5$ of a liquid sheet ruptures explosively. An example of an unstable liquid sheet with $W_e > 0.5$ is given in figure 3. Two branches of spatial amplification curves meet tangentially at the origin in the (k_r, k_i)-space of figure 3 (*a*). Figure 3 (*b*) shows how the upper and lower branches of curves coalesce at the origin when ω_r is decreased towards zero from a finite value. ω_i decreases (increases) with increasing k_r along the upper (lower) branch. Thus, the disturbances corresponding to the upper and lower branches propagate respectively in the upstream and downstream directions. Consequently, the upper branch with $k_i > 0$ and the lower branch with $k_i < 0$ both represent evanescent waves for finite k_r. A similar situation is encountered for the case of $Q \neq 0$ to be described in the next paragraph. Thus the theoretical results appear to contradict the known experimental

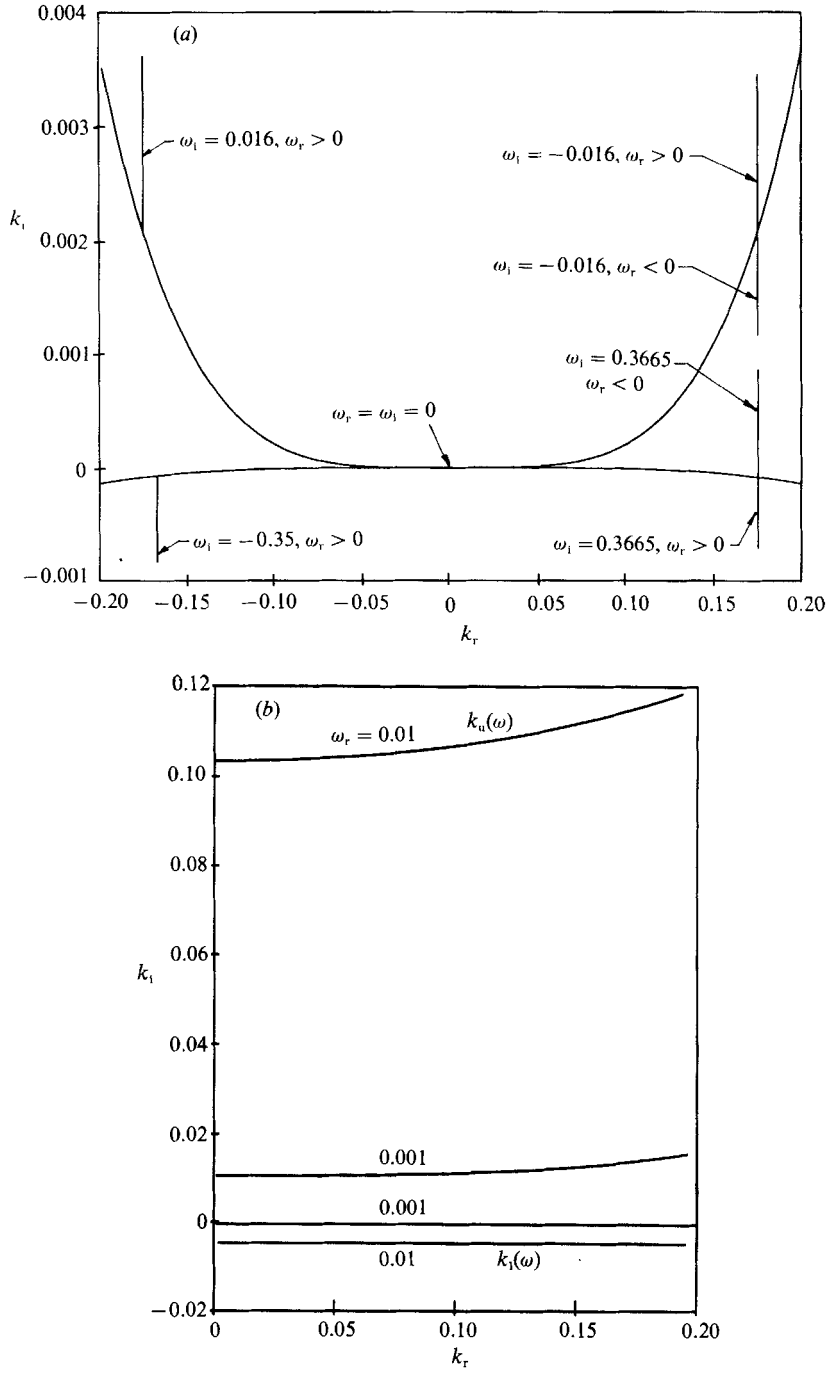

FIGURE 3. Sinuous mode. $Q = 0$, $W_e = 0.6$, $R = 1$. (*a*) Amplification curves; (*b*) formation of pinch-point singularity.

results for $W_e \geqslant 0.5$. An explanation is required. It is shown in the Appendix that the origin in figure 3 is a double pinch point where $\omega_r = 0$. While the double-pinch-point singularity is encountered at finite ω_r in the classical cases (Briggs 1964), it is encountered here at $\omega_r = 0$. In the usual absolute instability, the relevant Green's

function becomes unbounded as $\tau \to \infty$ (see for example, equation (15) of Bers 1983), when a pinch-point singularity is encountered. In the present case, the relevant Green's function is bounded, as shown in the Appendix, but is non-vanishing for all time and all spatial positions. Thus the evolution of disturbances does not satisfy the definition of convective stability (cf. (14) of Bers)

$$\lim_{\tau\to\infty} G(x,\tau) \to 0 \quad \text{for all } x.$$

Thus, the infinitely long wave for $W_e > 0.5$ is not evanescent. Nor does it satisfy the condition of convective instability (cf. (16*a*) and (16*b*) of Bers)

$$\lim_{\tau\to\infty} G(x,\tau) \to 0 \quad \text{for any finite } x$$

and

$$\lim_{\tau\to\infty} G(x_v,\tau) \to \infty,$$

where x_v is the distance measured from a reference frame moving with the group velocity. The evolution of disturbances is not that of an absolute instability either, since it does not satisfy the condition of absolute instability (cf. (15) of Bers)

$$\lim_{\tau\to\infty} G(x,\tau) \to \infty \quad \text{for all } x.$$

The evolution of the absolutely unstable disturbance and that of the present disturbance have an important common character: both of them remain non-vanishing for all time and all x. Note that the absolutely unstable disturbances are modified by nonlinear effects before they become unbounded and may become nonlinearly stable. The non-vanishing but bounded neutral disturbance we encountered here will also be modified by nonlinear effects at some finite time and may become nonlinearly unstable. It appears that the infinitely long neutral wave encountered here for $W_e > 0.5$ leads to nonlinear instability. It is interesting to note that the liquid sheet becomes unstable only with respect to a disturbance of infinitely long wavelength when $Q = 0$ and $W_e > 0.5$. This suggests that when the nonlinear effect is taken into account, the bifurcation is not that of Hopf. In fact experiments showed that when $W_e > 0.5$, the liquid sheet ruptures explosively without oscillation for a wide range of Q.

The presence of the ambient gas cannot remove the singularity at $k = \omega = 0$ when $W_e > 0.5$, as is demonstrated in figure 4 for a wide range of R. The branches of $\omega_r = 0$ in the region $k_r < 0$ are not shown in figure 4. As in figure 3, $\omega_i < 0$ (> 0) for the upper (lower) branch of the amplification curve in figure 4. Moreover, ω_i decreases (increases) along the upper (lower) branch with increasing k_r. Thus, the upper (lower) branch describes the upstream (downstream) propagating evanescent (spatially growing) waves. Again, the two branches coalesce at the origin where $\omega_r = 0$. Hence the large-time asymptotic behaviour of the disturbance at any *finite* x remains the same as that for the case of $Q = 0$. However, because the lower branch crosses the real k-axis, it can be shown that the disturbance becomes unbounded as $x \to -\infty$, $\tau \to \infty$ (Bers, equation (68)). It should be emphasized that the lower branch of the amplification curve in this figure does not signify convective instability, since the present large-time asymptotic behaviour does not satisfy the first condition of convective instability, i.e.

$$\lim_{\tau\to\infty} G(x,\tau) \to 0 \quad \text{for any finite } x.$$

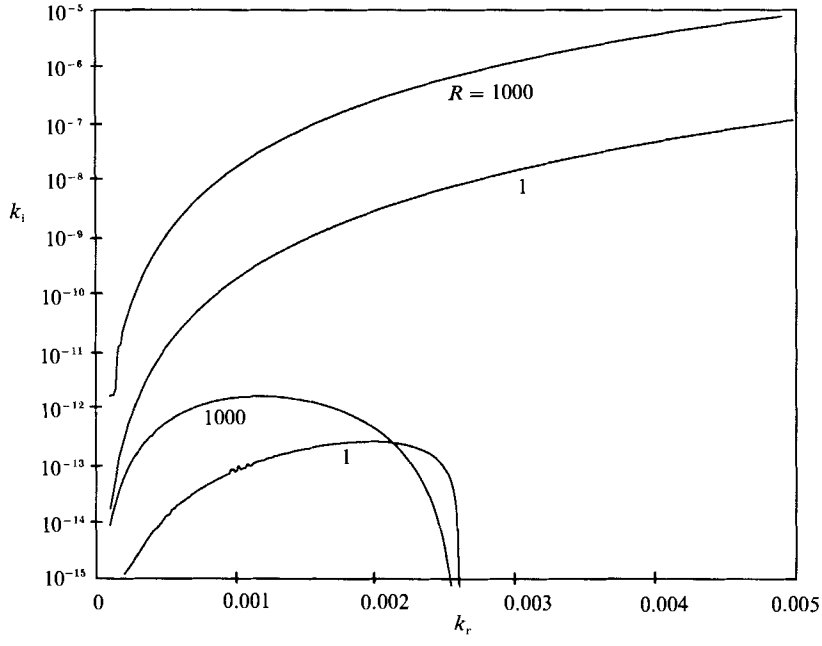

FIGURE 4. Sinuous mode. $Q = 1.3 \times 10^{-3}$, $W_e = 0.501$.

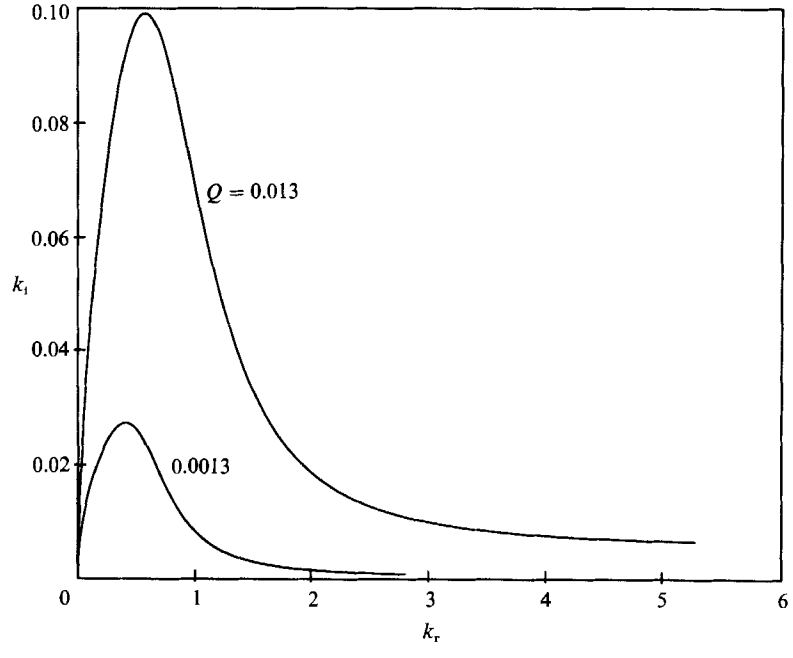

FIGURE 5. Effect of Q on convective instability, sinuous mode. $W_e = 10^{-4}$, $R = 1$.

We propose to call the instability we encounter here the pseudo-absolute instability, because the entire flow field is perturbed.

$Q = 0.0013$ and $Q = 0.013$ in figure 5 correspond respectively to the air-to-water density ratio at 1 and 10 times atmospheric pressure at room temperature. The

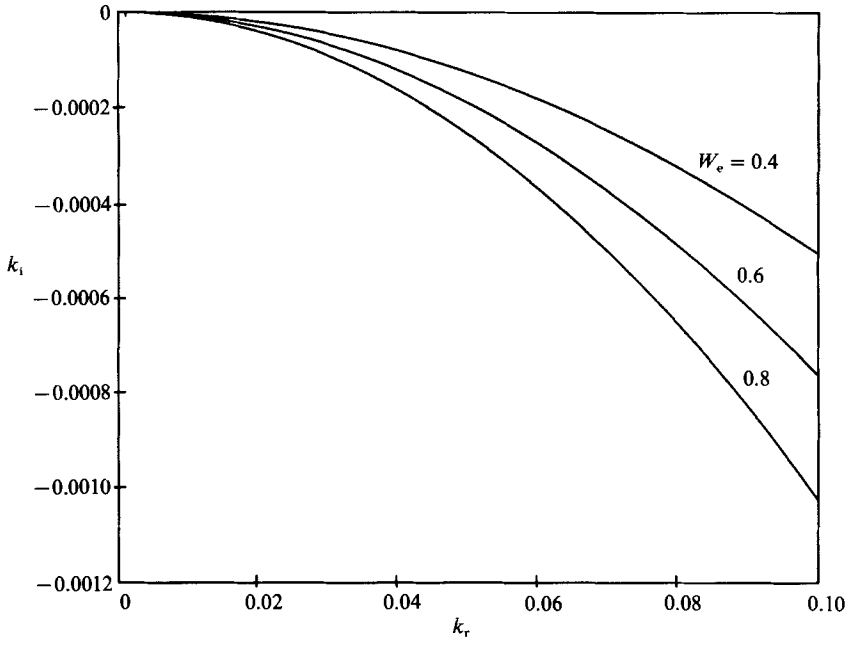

FIGURE 6. Asymptotic stability of varicose mode disturbances. $Q = 0$, $R = 1$.

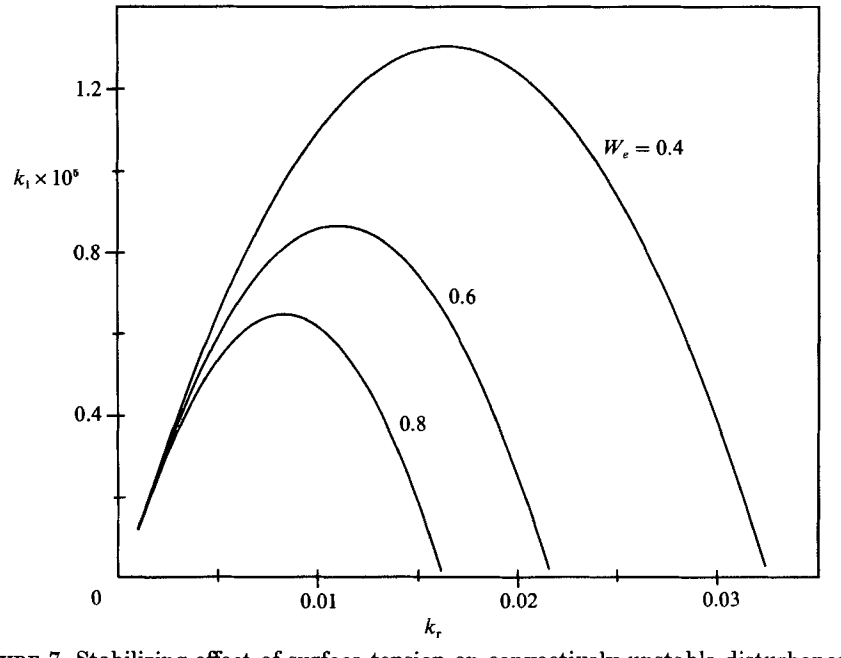

FIGURE 7. Stabilizing effect of surface tension on convectively unstable disturbances. $Q = 0.013$, $R = 1$, varicose mode.

spatial amplification curves $\omega_r = 0$ in this figure can be approached from $\omega_r > 0$ below the k_r-axis, without violating the causality condition. Moreover, ω_i increases with increasing k_r along these curves. Thus these curves signify the spatial amplification of convectively unstable sinuous disturbances propagating in the

$Q\times10^4$	$k_i\times10^8$	ω_i	$\dot{p}$	$\dot{p}_f$	$\dot{s}$	$\dot{\tau}$	$\dot{d}$
130	45891	−0.2478	1.24	0	184.55	−0.10	−85.68
1.3	49169	−0.2566	0.01	0	179.20	−0.10	−79.20

TABLE 1. Pseudo-absolute instability, $R = 100$, $W_e = 2.6$, $k_r = 0.2$

$W_e\times10^4$	k_r	k_i	ω_i	$\dot{p}$	$\dot{p}_f$	$\dot{s}$	$\dot{\tau}$	$\dot{d}$
13	0.508	0.0255	0.505	204.92	0.03	−104.35	0.01	−0.61
1.3	6.249	0.1261	6.242	312.43	0.55	−195.24	0	−17.74

TABLE 2. Convective instability, sinuous mode; $R = 5000$, $Q = 0.0013$

downstream direction (Bers 1983). Recall that it was shown in figure 2 that the sheet is stable when $Q = 0$, with the rest of flow parameters being the same. Thus, the presence of ambient gas causes the convective instability. No pseudo-absolute instability has been found for the varicose mode. In the absence of ambient gas, the varicose mode was found to be stable for a wide range of flow parameters. Figure 6 provides an example. However, in the presence of the ambient gas, the varicose mode is found to be convectively unstable in the same wide range of parameters. Figure 7 gives such an example. Figure 7 also shows that the surface tension is stabilizing, since the amplification rates decrease as W_e increases. The same dependence of growth rates on W_e is found for the sinuous mode when $W_e < 0.5$. Thus the convective instability is not caused by the surface tension. The growth rates of convectively unstable varicose disturbances are in general slightly smaller than that of the sinuous mode. The critical Weber number below which the instability is convective but above which it is pseudo-absolute is found to be 0.5 for R ranging from 0.1 to 10000 and Q from 0.00013 to 0.13.

Table 1 gives a typical energy budget for the case of pseudo-absolute instability. Tables 2 and 3 give typical energy budgets for the convective instability of the sinuous mode and the varicose mode respectively. The values of k_r, k_i and ω_i are all taken from the calculated spatial amplification curves $\omega_r = 0$. In particular, these values in tables 2 and 3 correspond to the maximum spatial growth rate on $\omega_r = 0$. While the positive dominant item in the pseudo-absolute instability case is the surface-tension-work term, that in the convective instability case is the terms due to the gas pressure work at the interface. Moreover, the surface-tension-work terms in the convective instability are negative. Thus while the surface tension work is responsible for the pseudo-absolute instability, the gas pressure work is responsible for the convective instability of both varicose and sinuous modes. It has been pointed out that the spatial growth rate of the varicose mode is smaller than that of sinuous mode for the same flow parameters. Comparing the viscous-dissipation and the surface-tension terms in tables 2 and 3, we find that the reason for this is that the varicose mode entails larger viscous dissipation and surface tension work. It can be seen that k_r in tables 2 and 3 scales with Q/W_e. The same situation has been found in other ranges of parameters.

$W_e \times 10^4$	k_r	k_i	ω_i	$\dot{p}$	$\dot{p}_f$	$\dot{s}$	$\dot{\tau}$	$\dot{d}$
13	0.74	0.0079	0.7397	403.84	0.32	−298.81	0	−5.35
1.3	6.30	0.1256	6.2927	317.67	0.59	−200.14	0	−18.11

TABLE 3. Convective instability, varicose mode; $R = 5000$, $Q = 0.0013$

5. Conclusion

It was shown in the last section that k_r corresponding to the maximum k_i scales with Q/W_e. This implies that in order to generate small droplets from atomizing a liquid sheet, one must use larger Q and smaller W_e, since the atomized droplets scale with the most amplified waves. Moreover, it is possible to atomize a liquid sheet to form droplets of radius, a, much smaller than the sheet thickness, because $a \sim \lambda \sim (1/k_r) \sim W_e/Q$, and the last ratio can be made quite small by use of a large sheet velocity, small surface tension or large ambient gas density. On the other hand, if one wishes to eliminate ripples in a curtain coating, one may operate in an environment without ambient gas. Then the curtain is stable if $W_e < 0.5$, which is easily satisfied in a high-speed curtain coating. The critical Weber numbers, W_{ec}, above which there is absolute instability and below which there is convective instability in a viscous jet were found to depend on Reynolds number by Leib & Goldstein (1986*a*, *b*) for the case of $Q = 0$ and by Lin & Lian (1989) for the case of $Q \neq 0$. Lin & Lian also showed the strong dependence of W_{ec} on Q. Here we found that the critical Weber number is insensitive to Q and R for a viscous sheet in an ambient gas. There is no explanation for this difference yet. The physical significance of pseudo- and genuine absolute instabilities in the context of nonlinear theory is yet to be explored. The nonlinear mechanism of direct resonance advanced by Akylas & Benney (1980) may be relevant. The effects of gas viscosity on the sheet stability remains unknown.

This work was supported in part by Grant No. DAALO3-89-K-0179 of ARO, Grant No. MSM-8817372 of NSF and a New York State Science Grant. This research was conducted using the Clarkson computer facility and the Cornell National Supercomputer Facility, a resource of the Center of Theory and Simulation in Science and Engineering, which receives major funding from NSF and IBM Corporation, with additional support from New York State and members of the Corporate Research Institute.

Appendix. Neutral instability

The Green's function corresponding to the dispersion relation (16) is given by (cf. eq. (6) of Bers 1983)

$$G(x,\tau) = \int \frac{\mathrm{d}\omega}{2\pi} \exp(\omega\tau) I(x,\omega), \quad I(x,\omega) = \int \frac{\exp(\mathrm{i}kx)\,\mathrm{d}k}{2\pi D(k,\omega)}, \tag{A 1}$$

where $D(k,\omega)$ is the left-hand side of (16), and the integrations in (A 1) are to be carried out along paths to be explained. It is easily verified from (16) that, at $k = k_0 = 0$, $\omega = \omega_0 = 0$

$$\frac{\partial D}{\partial k} = \frac{\partial D}{\partial \omega} = 0, \quad \text{but } \frac{\partial^2 D}{\partial k^2} \neq 0, \quad \frac{\partial^2 D}{\partial \omega^2} \neq 0, \quad \frac{\partial^2 D}{\partial \omega\, \partial k} \neq 0.$$

Taylor's series expansion of $D(k,\omega)$ about a pinch point (k_0,ω_0) gives to lowest order

$$(k-k_0)^2+\alpha(\omega-\omega_0)(k-k_0)+\beta(\omega-\omega_0)^2=0,$$

where
$$\alpha=\frac{\partial^2 D}{\partial\omega\,\partial k}\Big/\frac{\partial^2 D}{\partial k^2},\quad \beta=\frac{\partial^2 D}{\partial\omega^2}\Big/\frac{\partial^2 D}{\partial k^2}.$$

It follows that

$$k-k_0=[\gamma(\omega-\omega_0),\lambda(\omega-\omega_0)],$$

where
$$\gamma=\tfrac{1}{2}[-\alpha+(\alpha^2-4\beta)^{\frac{1}{2}}],\quad \lambda=\tfrac{1}{2}[-\alpha-(\alpha^2-4\beta)^{\frac{1}{2}}].$$

The double root at (k_0,ω_0) is formed by the coalescence of the upper branch of the amplification curve $k_u(\omega)$ and the lower branch $k_l(\omega)$ as ω_r is reduced from a positive value to zero as indicated in figure 3(*b*). Thus the dispersion relation near (k_0,ω_0) can be written as

$$D(k,\omega)=[k-k_u(\omega)][k-k_l(\omega)]L(k,\omega), \tag{A 2}$$

where $L(k,\omega)$ is regular near (k_0,ω_0) and

$$k_u=k_0+\gamma(\omega-\omega_0),\quad k_l=k_0+\lambda(\omega-\omega_0). \tag{A 3}$$

Since D^{-1} is single-valued and has only isolated poles and $\lim_{k\to\infty}D^{-1}\to 0$ faster than k^{-1}, $I(x,\omega)$ can be evaluated by closure in the upper k-plane for $x>0$ and in the lower k-plane for $x<0$. The theory of residues then gives

$$I(x,\omega)=\mathrm{i}u(x)\sum_{k_u}\exp[\mathrm{i}k_u(\omega)x]\Big/\left(\frac{\partial D}{\partial k}\right)_{k_u}+\mathrm{i}u(-x)\sum_{k_l}\exp[\mathrm{i}k_l(\omega)x]\Big/\left(\frac{\partial D}{\partial k}\right)_{k_l}, \tag{A 4}$$

where $u(x)$ is the unit step function in x. Substituting (A 2) and (A 3) into (A 4), we have

$$I(x,\omega)=\frac{\mathrm{i}u(x)\exp[\mathrm{i}k_u x]}{L(\gamma-\lambda)(\omega-\omega_0)}-\frac{-\mathrm{i}u(-x)\exp[\mathrm{i}k_l x]}{-L(\gamma-\lambda)(\omega-\omega_0)}+I_R(x,\omega), \tag{A 5}$$

where I_R represents the remaining summation in (A 4) which are not near k_0. Since $u(-x)=1-u(x)$, in the limit of $\omega\to\omega_0$, $k_u\to k_0$ and $k_l\to k_0$, (A 5) can be rewritten as

$$I(x,\omega)=\frac{\mathrm{i}\exp(\mathrm{i}k_0x)}{L(k_0,\omega_0)(\gamma-\lambda)(\omega-\omega_0)}+u(x)\left\{\frac{\partial[-\exp(\mathrm{i}kx)/\mathrm{i}L]}{\partial k}\right\}_{k_0,\omega_0}+I_R(x,\omega_0),$$

where the first term extends over all x, positive or negative, and has a pole of first order at $\omega=\omega_0$. The second term gives the residue in the second-order pole at $k=k_0$ and is regular in ω, as is the last term. With the expression of $I(x,\omega)$ near (k_0,ω_0) given above, the Green's function in (A 1) can be evaluated by use of the theory of residues,

$$G(x,\tau)\sim\int\exp(\mathrm{i}k_0x)\exp(\omega\tau)\,\mathrm{d}\omega/2\pi(\omega-\omega_0)$$

$$\sim\mathrm{i}\exp(\mathrm{i}k_0x+\omega_0\tau).$$

Here in this example $k_0=\omega_0=0$, and $G(x,\tau)$ remains non-vanishing for all time and all finite x.

REFERENCES

AKYLAS, T. R. & BENNEY, D. J. 1980 *Stud. Appl. Maths* **63**, 209.

ANTONIANDES, M. G. & LIN, S. P. 1980 *J. Colloid Interface Sci.* **77**, 583.

BERS, A. 1983 *Handbook of Plasma Physics*, Vol. 1, pp. 452–516. North-Holland.

BRIGGS, R. J. 1964 *Electron Stream Interaction with Plasmas*. MIT Press.

BROWN, D. R. 1961 *J. Fluid Mech.* **10**, 297.

CLARK, C. J. & DOMBROWSKI, N. 1972 *Proc. R. Soc. Lond.* A **329**, 467.

CRAPPER, G. D., DOMBROWSKI, N., JEPSON, W. P. & PYOTT, G. A. D. 1973 *J. Fluid Mech.* **57**, 671.

CRAPPER, G. D., DOMBROWSKI, N. & PYOTT, G. A. D. 1975 *Proc. R. Soc. Lond.* A **342**, 209.

CREIGHTON, N. 1989 Energy balance in breakup of liquid jets and curtains. M.S. thesis, Clarkson University.

LEIB, S. J. & GOLDSTEIN, M. E. 1986*a* *J. Fluid Mech.* **168**, 479.

LEIB, S. J. & GOLDSTEIN, M. E. 1986*b* *Phys. Fluids* **29**, 952.

KELLY, R. E., GOUSSIS, D. A., LIN, S. P. & HSU, F. K. 1989 *Phys. Fluids* A **1**, 819.

KISTLER, S. F. & SCRIVEN, L. E. 1984 *Intl J. Numer. Meth. Fluids* **4**, 207.

LIN, S. P. 1981 *J. Fluid Mech.* **104**, 111.

LIN, S. P. & LIAN, Z. W. 1989 *Phys. Fluids* A **1**, 490.

LIN, S. P. & ROBERTS, G. 1981 *J. Fluid Mech.* **112**, 443.

MULLER, D. E. 1956 *Mathematical Tables and Aid to Computation*, Vol. 10, pp. 208–230.

ROMBERS, S. 1984 *Problem Solving Software System for Mathematical and Statistical FORTRAN Programming*, I & II. IMSL.

TAYLOR, G. I. 1959*a* *Proc. R. Soc. Lond.* A **253**, 289.

TAYLOR, G. I. 1959*b* *Proc. R. Soc. Lond.* A **252**, 296.

TAYLOR, G. I. 1959*c* *Proc. R. Soc. Lond.* A **253**, 313.

TAYLOR, G. I. 1963 *The Scientific Papers of G. I. Taylor*, Vol. 3, No. 25. Cambridge University Press.

TOMOTIKA, S. 1934 *Proc. R. Soc. Lond.* A **146**, 501.

WEIHS, D. 1978 *J. Fluid Mech.* **87**, 289.